Taylor & Francis
Taylor & Francis Group

# An algorithm for synchronization of *in vivo* electroporation with ECG

B. MALI†, T. JARM†, F. JAGER‡ and D. MIKLAVČIČ†*

†Faculty of Electrical Engineering, University of Ljubljana, Tržaška 25, SI-1000 Ljubljana, Slovenia
‡Faculty of Computer and Information Science, University of Ljubljana, Tržaška 25, SI-1000 Ljubljana, Slovenia

The combined treatment of tumours in which delivery of a chemotherapeutic agent is followed by high voltage electroporation pulses has been termed electrochemotherapy. The electrochemotherapy of tumours located relatively close to the heart muscle can lead to fibrillation of the heart, especially if electroporation pulses are delivered in the vulnerable period of the heart or in coincidence with heart arrhythmias. We built an electroporation pulse delivery algorithm that enables safer use of electrochemotherapy. The algorithm is designed to deliver pulses outside the vulnerable period and to prevent pulses from being generated in the presence of heart arrhythmias. We evaluated the algorithm's performance using records of the Long-Term ST Database, thus simulating real-world conditions. The results of the evaluation, a sensitivity of 91.751%, a positive predictivity of 100.000% and a delivery error rate of 8.268% for electroporation pulse delivery (medians), suggest that the algorithm is accurate and appropriate for application in electrochemotherapy of tumours regardless of tumour location.

## 1. Introduction

The combined treatment in which delivery of a chemotherapeutic drug is followed by application of high voltage electric pulses locally to the tumour has been termed electrochemotherapy. The effect of local electropermeabilization of the cell membrane—also termed electroporation (EP)—enables entry of drug molecules into the cells and hence greater effectiveness of the tumour treatment. Electrochemotherapy has been successfully used for treatment of various cutaneous and subcutaneous tumours in different animal tumour models and in humans [1–4]. In these studies, a typical electrochemotherapy protocol involved eight EP pulses with amplitude approximately 1000 V, duration 100 $\mu$s, repetition frequency 1 Hz, and inter-electrode distance 8 mm. Beside this protocol, other protocols for delivery of EP pulses are either already being used or are expected to be developed and used in the future. For example, the protocol involving eight EP pulses at repetition frequency of 5 kHz has been suggested and is currently replacing the 1 Hz protocol due to a lesser discomfort and pain inflicted in patients [5]. Moreover, pulses of a much longer duration (on the order of milliseconds) are used for electrogene therapy [6]. Another

successful protocol for electrogene transfection relies on a combination of high voltage EP pulses with very long low voltage electrophoretic pulses (amplitude 50–100 V, duration 100 ms) in order to optimize gene transfer [7,8].

In spite of the increasing clinical use of electrochemotherapy this treatment has some minor side effects including transient lesions in areas in direct contact with the electrodes [9] and acute localized pain due to contraction of muscles in vicinity of the electrodes [2]. This induced contraction would become a problem if it were provoked in the heart muscle [10]. There is very little chance and absolutely no practical evidence that any electroporation protocol mentioned above could interfere with functioning of the heart when applied to cutaneous and subcutaneous tumours. However, a need for palliative treatment of internal tumours has emerged lately and treatment of internal tumours located close to the heart muscle would increase the probability of EP pulses interfering with the heart. The most dangerous possible interference is induction of ventricular fibrillation [10–12]. This issue is becoming increasingly important because new applications using endoscopic or surgical means to access internal tumours are being developed [13]. An algorithm for synchronization of EP pulse delivery with ECG to

---

*Corresponding author. Email: damijan@svarun.fe.uni-lj.si

maximize the safety for patients is needed before these applications can be realized.

Fibrillation of the heart can be induced if the amplitude of the externally applied electric pulses in a part of the heart is greater than the threshold level for fibrillation and if electrical stimulation is delivered during late atrial or ventricular systole—during the so-called vulnerable period [10,11,14]. For the ventricles, the vulnerable period is near the peak of the T wave and for the atria, it is probably in the S wave [15] (figure 1).

Although fibrillation can occur in normal and healthy hearts, it is more likely in hearts with structural or functional abnormalities [16]. Abnormalities of the heart rhythm (arrhythmias) are indicated by significant deviation of RR interval from its normal value [17]. During some arrhythmias the heart becomes significantly more susceptible to external stimuli due to a decreased threshold level for fibrillation. Therefore EP pulses coinciding with some arrhythmias could elicit fibrillation. This potential danger is most significant after the so-called premature response, the extrasystole [10].

In order to enable safer use of EP pulses during electrochemotherapy we developed an algorithm for synchronization of EP pulses with ECG. The algorithm allows EP pulses to be delivered only outside the vulnerable period of normal heartbeats (figure 1) and prevents the EP pulses from being generated in the presence of some common heart arrhythmias.

## 2. Methods

### 2.1. The algorithm

For application in electrochemotherapy the algorithm for QRS detection has to be simple enough for real-time realization, must enable early detection of QRS complex (i.e. detection based mainly on analysis of QR junction) and has to be able to distinguish well between



Figure 1. The vulnerable period for ventricles and atria.

normal and abnormal heartbeats. Based on the published algorithms [18] we developed a new algorithm that adequately fulfils these requirements. It is based on analysis of a single ECG lead at sampling frequency of 250 Hz and operates on individual signal samples in time-domain. It searches for the initial portion of the QRS complex, i.e. the ascendant QR junction slope and R wave peak, as early as possible prior to the vulnerable period, thus leaving enough time within QRS complex for electroporation pulse delivery.

During the electrochemotherapy protocol the patient is resting comfortably and thus the conditions for noise-free ECG signal prior to electroporation are fulfilled. Furthermore, the whole procedure of electrochemotherapy including the preparation of the patient is short (up to 10 minutes), while the electroporation procedure is even shorter (measured in seconds). The electrochemotherapy is performed only on patients without severe heart disease, so ECG signals without or with only minimal pathological changes can be expected. According to the electrochemotherapy protocol, there is currently no need for an algorithm for processing ECG signals containing distinctive noise and rapid changes of QRS complex morphology due to shifts of the mean electrical axis as a consequence of postural changes. To enable early detection of QRS complex an ECG lead with distinctive ascendant QR junction, high R wave amplitude and high dynamics within QRS complex in comparison to other parts of ECG signal is required. Typical standard ECG leads fulfilling these requirements include the chest lead $V_4$ and standard limb leads I and II. We use the term '$V_4$-like' lead for all leads suitable for our application. A '$V_4$-like' lead can easily be obtained in practice because it can be created by moving the ECG electrode to an arbitrary position, should none of the standard leads be appropriate.

The algorithm for synchronization of EP pulse delivery with ECG consists of two major components (the detection phase and the decision-making phase), which are preceded by the learning phase (figure 2).
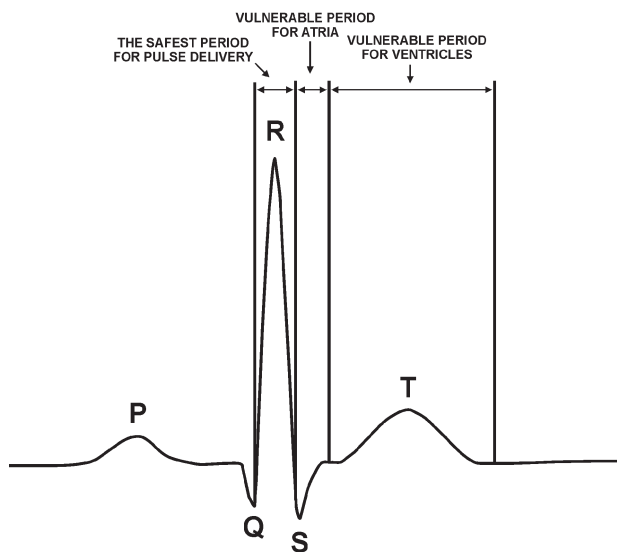
**2.1.1. The learning phase.** Adequate functioning of the algorithm is based on three main architecture parameters estimated during the learning phase from the ECG signal: the average value of the combination of the first and second derivative of the ECG signal ($\bar{Y}_{12}$); the running average R wave amplitude ($\bar{R}$); and the running average RR interval ($\overline{RR}$). Inter- and intra-record variability of these three parameters is very common. Therefore the algorithm determines their initial values during the learning phase. During this phase, an essentially noise-free ECG signal without heart arrhythmias or other heart abnormalities is required for fast adaptation to the given signal characteristics.

During part I of the learning phase (a 20-s interval) the value of the parameter $\bar{Y}_{12}$ is determined. This interval is divided into 20 equal subintervals. Within each subinterval, the maximum value of the slope parameter $Y_{12}$ (the combination of absolute values of first and second derivative of ECG signal) is determined using equations from [18]:
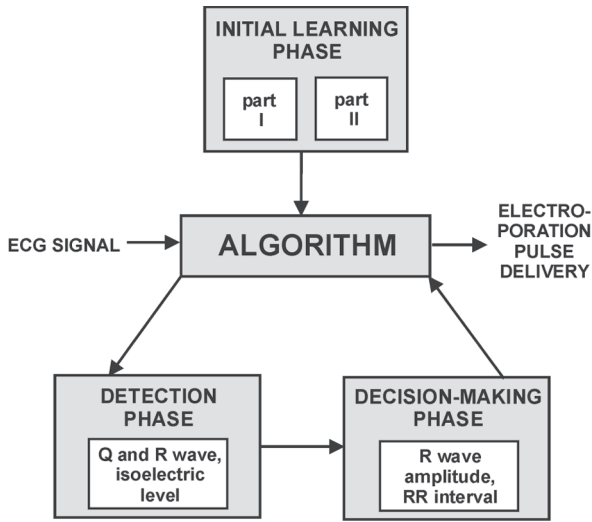
Figure 2. The structure of the algorithm.

$$Y_1(n) = \text{abs}[X(n+1) - X(n-1)], \qquad (1)$$

$$Y_2(n) = \text{abs}[X(n+2) - 2 \cdot X(n) + X(n-2)], \qquad (2)$$

$$Y_{12}(n) = 1.3 \cdot Y_1(n) + 1.1 \cdot Y_2(n), \qquad (3)$$

where $X(n)$ is the sequence of the ECG signal's samples. Normally the maximum values of $Y_{12}$ should be found on QRS complexes. The five largest and five smallest $Y_{12}$ values thus found are omitted and the average value ($\bar{Y}_{12}$) is calculated from the remaining 10 values.

During part II of the learning phase the algorithm detects consecutive QRS complexes by using the threshold value $Y_{th}$ (based on $\bar{Y}_{12}$) and estimates the other two parameters ($\bar{R}$ and $\overline{RR}$) with procedure described in next section. The threshold value $Y_{th}$ is taken as one seventh of $\bar{Y}_{12}$; this ratio was set empirically. The initial average R wave amplitude ($\bar{R}$) and RR interval ($\overline{RR}$) are calculated based on the latest 16 R wave amplitudes and the latest 8 RR intervals respectively. These averages, which are constantly being updated, are used in ECG analysis later on for calculation of several threshold parameters. These threshold parameters and their roles are described in the subsection on decision-making phase.

**2.1.2. The detection phase.** The algorithm for EP pulse delivery is based on accurate QRS complex detection, which is often difficult to achieve, since various sources of noise contamination and morphological differences in the ECG waveforms are frequently encountered [19]. The slope of the QR or RS interval of the QRS complex is a popular signal feature used to locate the QRS complex in many QRS detectors [18,20 – 22]. A real-time derivative algorithm that provides slope information is straightforward to implement but a slope alone is insufficient for accurate QRS complex detection. To achieve a reliable QRS detector performance, additional parameters often have to be extracted from the signal such as the R wave amplitude,

the width of the QRS complex, the RR interval, or the QRS energy [22].

Our QRS detector is an adaptation of the detector described in [18]. In order to improve the performance of the algorithm and to assure clear distinction between normal and abnormal individual heartbeats, we included additional signal features into consideration: the QR interval, the R wave amplitude and the RR interval. For implementation of such a detector the peaks of Q and R waves and the isoelectric level must be extracted from the ECG signal.

First, in order to locate the ascendant QR slope and R peak of the QRS complex, the algorithm searches for seven successive samples (set empirically and valid for a sampling frequency of 250 Hz) for which $Y_{12}$ is greater than or equal to $Y_{th}$ (figure 3). The sign of the first derivative must be positive in the first five samples of this set of seven, negative or equal to zero in the sixth sample and negative in the seventh sample. If all these conditions are fulfilled, it is very likely the algorithm has located the R wave. All together 11 successive signal samples (marked with a 'star' symbol in figure 3) are used for the procedure of finding $Y_{12}$ in seven successive samples.

Second, the peak of R wave is sought for. The peak of R wave corresponds to the sample with maximum amplitude among the 11 samples used so far (figure 3). Third, the Q peak is detected. The algorithm calculates the first derivative backwards from the R peak for 80 ms until it finds four successive signal samples among which the first (counted from the left to right) has either a negative or zero first derivative and the other three have a positive first derivative (figure 3). The Q peak thus corresponds to either the first or the second of these four samples. After this, the QR interval can be defined. Fourth, the correctness of the R wave location is further assured by comparing the QR interval to typical normal QR interval, which is approximately 0.03 s long [10]. If the current QR interval is not within the 0.02 – 0.10 s range (set empirically), the analysis of the current heartbeat is discontinued and the next normal heartbeat is sought for. The length of QR interval also helps in distinguishing the QRS complex from high frequency noise. Fifth, the flattest part of the PQ segment, termed the isoelectric level, is determined. The algorithm searches for the isoelectric level backwards from the Q peak but only up to 108 ms backwards from the R peak [23]. For each series of five successive samples within this interval the algorithm calculates the average amplitude value and the total deviation value. The average value of the samples that have the minimal total deviation from the average value is taken as the isoelectric level. Finally, the R wave amplitude can be calculated as the difference between the R peak value and the isoelectric level.

**2.1.3. The decision-making phase.** During the decision-making phase, the algorithm decides about delivery of the EP pulses with respect to deviations of R wave amplitude and heart rate (indicated by the RR interval) of individual heartbeats from average values of $\bar{R}$ and $\overline{RR}$.

If the value of amplitude of the current QRS complex is within $\pm 30\%$ of $\bar{R}$ and if the value of the current RR interval is within $-7\%$ to $+15\%$ of $\overline{RR}$, the current QRS
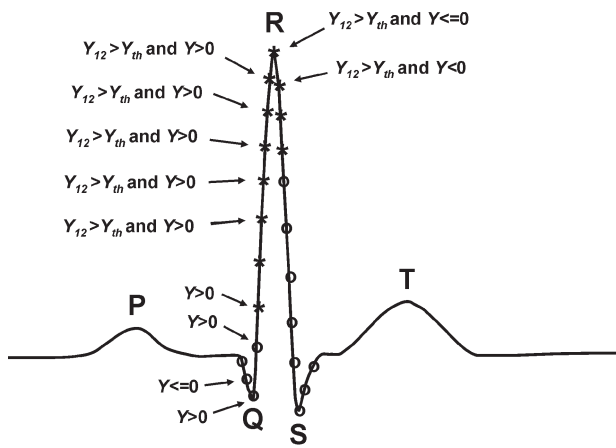
Figure 3. The conditions for detection of R and Q wave. For R wave detection the value of $Y_{12}$ for seven successive samples has to be larger than the threshold value $Y_{th}$ and at the same time the value of first derivative ($Y$) must be positive for the first five, negative or zero for the sixth, and negative for the seventh sample. Eleven successive samples (marked with a 'star' symbol) are used for this procedure. For Q wave detection the first value of $Y$ among four successive $Y$ values must be negative or zero and the remaining three $Y$ values positive.

complex is considered non-pathological, i.e. normal. Therefore, the algorithm would deliver the EP pulse. These threshold values for EP pulse delivery have to follow slow morphology changes of the signal, which occur normally in any ECG signal. Therefore $\bar{R}$ and $\overline{RR}$ values are calculated as the moving average of the 16 and eight most recent values, respectively, that also fall within the following threshold values for updating. If the value of amplitude of the current QRS complex is within $\pm 40\%$ of $\bar{R}$ and if the value of the current RR interval is within $\pm 25\%$ of $\overline{RR}$, the current averages $\bar{R}$ and $\overline{RR}$ are updated. The expression of all threshold values in terms of percentages of $\bar{R}$ and $\overline{RR}$ that we report here are based on empirical evaluation of the algorithm's performance.

We incorporate only eight RR intervals in the running average $\overline{RR}$ (in comparison with 16 R wave amplitudes used in the running average $\bar{R}$) because the RR interval is expected to be less steady than the R wave amplitude in normal heartbeats. Therefore it is possible to account for relatively rapid but normal changes in the rhythm of the heart. This feature is of great importance for proper distinguishing between normal heartbeat intervals and heart arrhythmias. The threshold values for updating are set wider apart than the threshold values for the EP pulse delivery. The reason for this is that we must be extremely cautious about the EP pulse delivery and thus be convinced that we are really dealing with a non-pathological heartbeat. While inclusion of an abnormal heartbeat in calculation of running averages $\bar{R}$ and $\overline{RR}$ is not critical (e.g. one abnormal value among 15 or seven normal ones, respectively), delivery of an EP pulse in such conditions could be dangerous.

The possibility of the onset of various arrhythmias is of predominant concern when deciding whether to deliver an EP pulse or not. Therefore, even when our QRS detector finds a QRS complex, the algorithm would not allow for the EP pulse delivery if the current RR interval significantly deviates from $\overline{RR}$. The allowed deviation of current RR interval is $-7\%$ to $+15\%$ from $\overline{RR}$. The lower threshold was chosen because extrasystoles can occur as little as 7–10% prematurely [10] and we absolutely want to avoid EP pulse delivery in the case of extrasystoles. Initially the upper threshold was set to $+7\%$ but this resulted in an unacceptable decrease in the number of delivered pulses. Since the heartbeats delayed for more than 7% are not problematic for our application, we found the upper threshold of $+15\%$ to be appropriate.

## 2.2. *Evaluation of the algorithm*

**2.2.1. ECG database.** We evaluated the performance of our algorithm using selected records of the Long-Term ST Database (LTST DB) [24]. The LTST DB contains approximately 24-hour long ambulatory Holter records reflecting the real-world clinical environment with all heartbeats classified by experts. Therefore all usual daily activities of the patient are reflected in ECG signals, which also contain abnormal heartbeats of various pathological backgrounds.

Since many records are not 'V4-like' and since we do not expect extreme conditions with respect to abnormal heartbeats, nor severe levels of noise in the input signals during electrochemotherapy protocol, we selected only 42 records from the pool of 86 records of the LTST DB. First, we excluded the records containing QRS complex conduction changes (s20531, s20541, s20551, s30721) and unreadable intervals (s20291, s20561, s20571, s20601, s20621, s30761, s30801). The electroporation pulse delivery would not be started or would be terminated under such conditions in clinical practice. Then we excluded non-'V4-like' ECG signals (s20191, s20221, s20251, s20301, s20311, s20341, s20391, s20431, s20461, s20481, s20581, s20591, s20611, s20641, s20651, s30661, s30681, s30771, s30781). During the electrochemotherapy, a requirement for accurate electroporation pulse delivery is a suitable QRS complex morphology. Then, with respect to graphic trends of diagnostic and morphology parameters of the database [24], we excluded the records containing significant axis shifts and consequently rapid significant changes in the QRS complex morphology (s20051, s20201, s20271, s20272, s20273, s20274, s20331, s20501, s30731, s30732), and records containing considerable noise intervals (s20041, s20511, s20521, s20161). The remaining records and ECG leads used to evaluate the performance of our algorithm are evident from table 1.

In the process of developing the algorithm we used two two-hour-long sections from the beginning of two ECG signals from the LTST DB. The first section from signal s20011 features mostly normal heartbeats and only an insignificant number of pathological heartbeats (see table 1). The second section from signal s20101 includes a lot of

Table 1. ECG signals from the LTST DB, ECG lead used, number of heartbeats of particular type, results of QRS detection and results of EP pulse delivery†.

| Signal name | Signal number | Lead name | $N$ | $V$ | $S$ | $N_d$ | $TP$ | $FN$ | $FP$ | $Se$ (%) | $+P$ (%) | $DER$ (%) | $N_p$ | $TP_p$ | $FN_p$ | $FP_p$ | $V_p$ | $S_p$ | $Se_p$ (%) | $+P_p$ (%) | $DER_p$ (%) |
|---|---|---|---|---|---|---|---|---|---|---|---|---|---|---|---|---|---|---|---|---|---|
| s20011 | 0 | ML2 | 100028 | 2 | 23 | 100014 | 99883 | 131 | 0 | 99.869 | 100.000 | 0.131 | 99989 | 97201 | 2788 | 1 | 0 | 1 | 97.212 | 99.999 | 2.789 |
| s20021 | 1 | $V_4$ | 88755 | 138 | 69 | 88923 | 88589 | 334 | 1 | 99.624 | 99.999 | 0.377 | 88716 | 85642 | 3074 | 1 | 0 | 1 | 96.535 | 99.999 | 3.466 |
| #s20031 | 1 | x | 107069 | 1 | 2430 | 109460 | 109201 | 259 | 1 | 99.763 | 99.999 | 0.238 | 107028 | 101540 | 5488 | 1 | 0 | 1 | 94.872 | 99.999 | 5.129 |
| s20061 | 0 | ML2 | 117114 | 776 | 4 | 117873 | 117069 | 804 | 0 | 99.318 | 100.000 | 0.682 | 117092 | 99562 | 17530 | 0 | 0 | 0 | 85.029 | 100.000 | 14.971 |
| s20071 | 0 | ML2 | 85745 | 5 | 0 | 85714 | 85437 | 277 | 0 | 99.677 | 100.000 | 0.323 | 85701 | 82602 | 3099 | 0 | 0 | 0 | 96.384 | 100.000 | 3.616 |
| #s20081 | 0 | ML2 | 111662 | 1292 | 2 | 112936 | 110130 | 2806 | 1 | 97.515 | 99.999 | 2.485 | 111642 | 96589 | 15053 | 0 | 0 | 0 | 86.517 | 99.999 | 13.483 |
| s20091 | 0 | ML2 | 111565 | 0 | 5 | 111331 | 111321 | 10 | 0 | 99.991 | 100.000 | 0.009 | 111326 | 90499 | 20827 | 0 | 0 | 0 | 81.292 | 100.000 | 18.708 |
| #s20101 | 0 | ML2 | 70504 | 7081 | 48 | 77978 | 70357 | 7621 | 0 | 90.227 | 100.000 | 9.773 | 70849 | 60656 | 10193 | 1 | 0 | 1 | 85.613 | 99.998 | 14.388 |
| s20111 | 0 | ML2 | 85186 | 3 | 75 | 85218 | 84806 | 412 | 0 | 99.517 | 100.000 | 0.483 | 85139 | 83314 | 1825 | 0 | 0 | 0 | 97.856 | 100.000 | 2.144 |
| s20121 | 0 | ML2 | 84927 | 580 | 19 | 85490 | 84358 | 1132 | 0 | 98.676 | 100.000 | 1.324 | 84891 | 83361 | 1530 | 0 | 0 | 0 | 98.198 | 100.000 | 1.802 |
| s20131 | 0 | ML2 | 105765 | 495 | 33 | 106256 | 105338 | 918 | 0 | 99.136 | 100.000 | 0.864 | 105727 | 103984 | 1743 | 0 | 0 | 0 | 98.351 | 100.000 | 1.649 |
| s20141 | 0 | ML2 | 116625 | 0 | 49 | 116630 | 116577 | 53 | 0 | 99.955 | 100.000 | 0.045 | 116581 | 112825 | 3756 | 3 | 0 | 3 | 96.778 | 99.997 | 3.224 |
| s20151 | 0 | $V_4$ | 79492 | 166 | 6 | 79638 | 79437 | 201 | 0 | 99.748 | 100.000 | 0.252 | 79466 | 75596 | 3870 | 0 | 0 | 0 | 95.130 | 100.000 | 4.870 |
| s20171 | 0 | $V_4$ | 126515 | 9 | 2 | 126481 | 126173 | 308 | 0 | 99.756 | 100.000 | 0.244 | 126470 | 115118 | 11352 | 0 | 0 | 0 | 91.024 | 100.000 | 8.976 |
| s20211 | 1 | $V_4$ | 106836 | 125 | 15 | 106913 | 104140 | 2773 | 2 | 97.406 | 99.998 | 2.596 | 106772 | 93166 | 13606 | 0 | 0 | 0 | 87.257 | 100.000 | 12.743 |
| s20221 | 0 | ML2 | 99840 | 17 | 2 | 99793 | 99531 | 262 | 1 | 99.737 | 99.999 | 0.264 | 99773 | 81670 | 18103 | 0 | 0 | 0 | 81.856 | 100.000 | 18.144 |
| s20231 | 0 | ML2 | 103061 | 2 | 34 | 103057 | 100346 | 2711 | 0 | 97.369 | 100.000 | 2.631 | 103018 | 81352 | 21666 | 0 | 0 | 0 | 78.969 | 100.000 | 21.031 |
| s20241 | 0 | ML2 | 92424 | 6 | 3 | 92381 | 92151 | 230 | 0 | 99.751 | 100.000 | 0.249 | 92366 | 71851 | 20515 | 0 | 0 | 0 | 77.789 | 100.000 | 22.211 |
| s20261 | 0 | x | 101491 | 746 | 71 | 102270 | 101508 | 762 | 0 | 99.255 | 100.000 | 0.745 | 101451 | 94723 | 6728 | 5 | 5 | 0 | 93.368 | 99.995 | 6.637 |
| s20281 | 0 | x | 72989 | 0 | 87 | 73041 | 72979 | 62 | 0 | 99.915 | 100.000 | 0.085 | 72954 | 70920 | 2034 | 0 | 0 | 0 | 97.212 | 100.000 | 2.788 |
| s20321 | 0 | $V_4$ | 91679 | 201 | 49 | 91888 | 91507 | 381 | 3 | 99.585 | 99.997 | 0.418 | 91638 | 78369 | 13269 | 0 | 0 | 0 | 85.520 | 100.000 | 14.480 |
| s20351 | 0 | x | 118847 | 796 | 9 | 119607 | 118736 | 871 | 0 | 99.272 | 100.000 | 0.728 | 118802 | 116595 | 2207 | 0 | 0 | 0 | 98.142 | 100.000 | 1.858 |
| s20361 | 0 | x | 105658 | 11 | 18 | 105650 | 105169 | 481 | 0 | 99.545 | 100.000 | 0.455 | 105621 | 102349 | 3272 | 1 | 0 | 1 | 96.902 | 99.999 | 3.099 |
| s20371 | 0 | x | 95733 | 5 | 12 | 95710 | 95602 | 108 | 1 | 99.887 | 99.999 | 0.114 | 95693 | 92693 | 3000 | 0 | 0 | 0 | 96.865 | 100.000 | 3.135 |
| s20381 | 0 | x | 102904 | 53 | 15 | 102924 | 94375 | 8549 | 9 | 91.694 | 99.999 | 8.307 | 102856 | 90754 | 12102 | 6 | 4 | 2 | 88.234 | 99.993 | 11.772 |
| s20401 | 1 | x | 77269 | 61 | 3 | 77299 | 77160 | 139 | 1 | 99.820 | 100.000 | 0.180 | 77235 | 62700 | 14535 | 0 | 0 | 0 | 81.181 | 100.000 | 18.819 |
| s20411 | 1 | x | 84385 | 23 | 299 | 84672 | 84543 | 129 | 3 | 99.848 | 99.996 | 0.152 | 84350 | 83133 | 1217 | 3 | 3 | 3 | 98.557 | 99.996 | 1.446 |
| #s20421 | 1 | x | 87657 | 93 | 5211 | 92920 | 90719 | 2201 | 0 | 97.631 | 100.000 | 2.369 | 87614 | 79894 | 7720 | 3 | 0 | 3 | 91.189 | 99.996 | 8.815 |
| #s20441 | 1 | x | 89666 | 3436 | 23 | 93078 | 88884 | 4194 | 0 | 95.494 | 100.000 | 4.506 | 89617 | 80678 | 8939 | 2 | 0 | 2 | 90.025 | 99.998 | 9.977 |
| s20451 | 0 | x | 88006 | 3 | 46 | 88021 | 79336 | 8685 | 3 | 90.133 | 99.996 | 9.870 | 87972 | 71968 | 16004 | 1 | 0 | 1 | 81.808 | 99.999 | 18.193 |
| s20471 | 0 | $V_4$ | 115231 | 61 | 10 | 115258 | 115078 | 180 | 1 | 99.844 | 99.999 | 0.157 | 115187 | 107227 | 7960 | 0 | 0 | 0 | 93.089 | 100.000 | 6.911 |
| s20491 | 0 | $V_4$ | 96128 | 775 | 47 | 96911 | 92174 | 4737 | 9 | 95.112 | 99.990 | 4.897 | 96088 | 75055 | 21033 | 1 | 0 | 1 | 78.111 | 99.999 | 21.890 |
| s20631 | 0 | $V_4$ | 100030 | 0 | 6 | 99994 | 95897 | 4097 | 1 | 95.903 | 99.999 | 4.098 | 99988 | 83912 | 16076 | 0 | 0 | 0 | 83.922 | 100.000 | 16.078 |
| s20671 | 1 | $V_5$ | 98545 | 350 | 143 | 99040 | 98547 | 493 | 3 | 99.502 | 99.997 | 0.501 | 98547 | 90110 | 8437 | 16 | 0 | 16 | 91.439 | 99.982 | 8.578 |
| s30691 | 1 | A-S | 101655 | 1 | 27 | 101644 | 98794 | 2850 | 2 | 97.196 | 99.998 | 2.806 | 101616 | 95399 | 6217 | 0 | 0 | 0 | 93.882 | 100.000 | 6.118 |
| s30701 | 2 | A-I | 107061 | 0 | 17 | 107036 | 104129 | 2907 | 0 | 97.284 | 100.000 | 2.716 | 107019 | 101684 | 5335 | 0 | 0 | 0 | 95.015 | 100.000 | 4.985 |
| #s30711 | 1 | A-S | 134278 | 19041 | 10 | 153227 | 19040 | 134187 | 0 | 12.426 | 100.000 | 87.574 | 134176 | 18671 | 115505 | 0 | 0 | 0 | 13.915 | 100.000 | 86.085 |
| s30741 | 0 | E-S | 123461 | 0 | 0 | 123419 | 123116 | 303 | 0 | 99.754 | 100.000 | 0.246 | 123419 | 119692 | 3727 | 0 | 0 | 0 | 96.980 | 100.000 | 3.020 |
| s30742 | 0 | E-S | 113767 | 0 | 0 | 113696 | 113591 | 105 | 0 | 99.908 | 100.000 | 0.092 | 113696 | 109954 | 3742 | 0 | 0 | 0 | 96.709 | 100.000 | 3.291 |
| #s30751 | 2 | A-I | 102514 | 3476 | 66 | 106017 | 102306 | 3711 | 1 | 96.500 | 99.999 | 3.501 | 102475 | 94341 | 8134 | 20 | 20 | 0 | 92.062 | 99.979 | 7.957 |
| #s30752 | 1 | A-S | 114473 | 5991 | 81 | 120414 | 90237 | 30177 | 0 | 74.939 | 100.000 | 25.061 | 114342 | 78165 | 36177 | 53 | 53 | 0 | 68.361 | 99.932 | 31.686 |
| s30791 | 1 | A-S | 100325 | 57 | 99 | 100433 | 88245 | 12188 | 0 | 87.865 | 100.000 | 12.135 | 100214 | 84629 | 15585 | 0 | 0 | 0 | 84.448 | 100.000 | 15.552 |

Table 1 (*continued*)

| Signal name | Signal number | Lead name | $N$ | $V$ | $S$ | $N_d$ | $TP$ | $FN$ | $FP$ | $Se$ (%) | $+P$ (%) | $DER$ (%) | $N_p$ | $TP_p$ | $FN_p$ | $FP_p$ | $V_p$ | $S_p$ | $Se_p$ (%) | $+P_p$ (%) | $DER_p$ (%) |
|---|---|---|---|---|---|---|---|---|---|---|---|---|---|---|---|---|---|---|---|---|---|
| Total | – | – | 4216865 | 45878 | 9168 | 4270255 | 4026516 | 243739 | 31 | – | – | – | 4215116 | 3700143 | 514973 | 118 | 82 | 36 | – | – | 1.446 |
| Min | – | – | 70504 | 0 | 0 | 73041 | 19040 | 10 | 0 | 12.426 | 99.990 | 0.009 | 70849 | 18671 | 1217 | 0 | 0 | 0 | 13.915 | 99.932 | 3.335 |
| 25% | – | – | 88982 | 2 | 6 | 92011 | 88331 | 237 | 0 | 97.218 | 99.999 | 0.244 | 88941 | 80090 | 3386 | 0 | 0 | 0 | 84.593 | 99.999 | 8.268 |
| Median | – | – | 100908 | 55 | 21 | 101039 | 97222 | 628 | 0 | 99.410 | 100.000 | 0.591 | 100833 | 87876 | 8047 | 0 | 0 | 0 | 91.751 | 100.000 | 15.407 |
| 75% | – | – | 110441 | 559 | 62 | 110863 | 105296 | 2893 | 1 | 99.756 | 100.000 | 2.783 | 110252 | 98972 | 15452 | 1 | 0 | 1 | 96.761 | 100.000 | 86.085 |
| Max | – | – | 134278 | 19041 | 5211 | 153227 | 126173 | 134187 | 9 | 99.991 | 100.000 | 87.574 | 134176 | 119692 | 115505 | 53 | 53 | 16 | 98.557 | 100.000 | 11.584 |
| Mean | – | – | 100402 | 1092 | 218 | 101673 | 95869 | 5803 | 1 | 95.365 | 99.999 | 4.635 | 100360 | 88099 | 12261 | 3 | 2 | 1 | 88.419 | 99.997 | 13.870 |
| St. dev. | – | – | 14491 | 3228 | 873 | 15559 | 18177 | 20940 | 2 | 13.902 | 0.002 | 13.902 | 14461 | 17946 | 17996 | 9 | 9 | 3 | 13.869 | 0.011 | |

†$N$ = normal heartbeat; $V$ = ventricular premature or ectopic beat; $S$ = supraventricular premature or ectopic beat; $N_d$ = total number of possible detected QRS complexes (normal and abnormal), the sum of $TP$ and $FN$; $TP$ = true positive for QRS detection (the number of correctly detected QRS complexes); $FN$ = false negative for QRS detection (the number of missed QRS complexes); $FP$ = false positive for QRS detection (the number of false QRS detections); $Se$ = sensitivity for QRS detections; $+P$ = positive predictivity for QRS detection; $DER$ = detection error rate for QRS detection; $N_p$ = total number of normal QRS complexes (total number of possible delivered EP pulses), the sum of $TP_p$ and $FN_p$; $TP_p$ = true positive for EP pulses (the number of EP pulses delivered at correctly detected normal QRS complexes); $FN_p$ = false negative for EP pulses (the number of correctly detected normal QRS complexes. where no EP pulse was delivered); $FP_p$ = false positive for EP pulses (the number of EP pulses delivered in absence of correctly detected normal QRS complexes); $V_p$ = number of EP pulses delivered within ventricular premature beat; $S_p$ = number of EP pulses delivered within supraventricular premature or ectopic beat; $Se_p$ = sensitivity for EP pulses; $+P_p$ = positive predictivity for EP pulses; $DER_p$ = delivery error rate for EP pulses; # = ECG signals with relatively poor values of performance metrics due to the presence of many heart arrhythmias; $x$ = lead of ECG record unknown.

heart arrhythmias (see table 1) and other heart rate-related changes. Since the sections used for the development of the algorithm were only two-hour parts of the recorded signals, we included whole signals in the evaluation of the algorithm as well.

**2.2.2. Performance metrics.** For evaluation of QRS complex detection we calculated the following scores for each record: $N_d$, *TP, FN* and *FP* (for definitions see table 1). Based on these scores obtained with a beat-by-beat comparison of the results of our algorithm with true human-expert annotations of the heartbeats defined in the LTST DB, we calculated standard performance measures of the algorithm: sensitivity (*Se*), positive predictivity ( $+ P$ ) and detection error rate (*DER*) for QRS detection (equations (4)–(6), respectively). The performance measures for an ideal QRS detector would be $Se = 100\%$, $+ P = 100\%$ and $DER = 0\%$.

$$Se(\%) = \frac{TP}{N_d} \cdot 100, \qquad (4)$$

$$+P(\%) = \frac{TP}{TP + FP} \cdot 100, \qquad (5)$$

$$DER(\%) = \frac{FP + FN}{N_d} \cdot 100. \qquad (6)$$

For evaluation of EP pulse delivery we calculated the following scores for each record: $N_p$, $TP_p$, $FN_p$ and $FP_p$ (for definitions see table 1). Based on these scores and in absence of any standard performance metrics for EP pulse delivery, we calculated the performance measures analogous to QRS detection metrics: sensitivity ($Se_p$), positive predictivity ( $+ P_p$ ) and delivery error rate ($DER_p$) for EP pulses. The performance measures for an ideal algorithm for EP pulse delivery would be $Se_p = 100\%$, $+ P_p = 100\%$ and $DER_p = 0\%$.

### 2.3. Programming

The algorithm itself and all routines for evaluation of performance were written in ANSI C programming language and implemented on a PC platform. In the future this will enable an easy translation of the algorithm into assembly language and its application in the existing microprocessor-driven instrument for clinical use of electroporation.

### 3. Results

The performance of the algorithm summarized in table 1 shows the ability of the algorithm to detect QRS and to deliver EP pulses correctly. Since data pertaining to individual records were not normally distributed, we provide a statistical summary of the results using both the mean and standard deviation and the median and quartile values. However, when we say 'on average' in the text we are always referring to median values, which are more representative of the middle of the sample and population than the mean values.

On average, the algorithm correctly detected 99.410% of all QRS complexes. The total number of erroneously detected QRS complexes was only 31, which is a very small number compared to the total number of QRS complexes (over $4 \times 10^6$). The detection error rate for QRS detection (*DER*) was 0.591% on average. Average positive predictivity for QRS detection ( $+ P$ ) was 100.000%.

On average, the algorithm correctly delivered EP pulses in 91.751% of normal QRS complexes. The value of delivery error rate for EP pulses ($DER_p$) was 8.268% and the value of positive predictivity for EP pulses ( $+ P_p$ ) 100.000% on average.

### 4. Discussion

The algorithm for synchronization of EP with ECG reliably detected QRS complexes in all 42 'V$_4$-like' signals from the LTST DB (see table 1). The algorithm allowed for EP pulse delivery for each correctly identified heartbeat if no abnormalities were detected. The performance of our algorithm (see §2.2.2) approached the ideal level at a degree similar to that of some other detectors with comparably simple algorithms [19,25]. The records with poorest results of our algorithm (large *DER*) contain very unstable R wave amplitudes, very unstable RR intervals and a transient appearance of high frequency noise with amplitudes similar to the R wave. At this preliminary stage of development our algorithm is not well suited to deal with signals that are largely nonstationary or have very low signal-to-noise ratio. However, due to its conservative nature the algorithm deals well with mildly nonstationary parts of the signal or transient onsets of noise contamination with low amplitudes, which were occasionally encountered in most of the signals used in evaluation of the algorithm. Moreover, many of the false negative detections (*FN*) were due to very strict requirements for no false positive detections (*FP*).

The algorithm could deliver the EP pulse either before vulnerable period or after it. Since the vulnerable period can sometimes be prolonged (e.g. after premature response) [10], it is obviously more reasonable to deliver the EP pulse before rather than after the onset of vulnerable period. Therefore, the most appropriate moment for EP pulse delivery is immediately after the QRS detection but still within the QRS complex. The delivery of EP pulses during vulnerable period of the atria does not present a serious threat for the patient's life. The haemodynamic effects of atrial flutter and fibrillation, which could be potentially caused by EP pulse delivery during vulnerable period for atria, are only slight and the patients are frequently unaware of these arrhythmias [10]. Bearing these facts in mind we can conclude that the time reserve for safe EP pulse delivery after the QRS detection and before the onset of vulnerable period for ventricles is approximately 60 ms and is long enough for safe EP pulse delivery even if we want to avoid the vulnerable period of atria as well.

Our main concern is to avoid, at any cost, delivery of EP pulses at the moments of potential danger for the patient. The algorithm fulfilled this requirement excellently as

indicated by practically ideal $+P_p$ values (table 1). We made our algorithm deliberately more conservative than would be necessary if the purpose was solely to detect QRS complexes. It is completely acceptable to miss some normal heartbeats (increase in $FN$ and $FN_p$) as long as no EP pulse is delivered when it absolutely should not be ($FP_p = 0$!). Upon careful examination, we found 16 ECG signals in which the $FP_p$ was not zero. The erroneously delivered pulses (there were 118 such pulses in comparison to approximately $3.7 \times 10^6$ correctly delivered EP pulses) coincided with appearance of some extrasystoles of either supraventricular or ventricular origin. The reason for $FP_p$ is mainly in morphology (e.g. the heartbeats without distinct P wave) and the time of appearance of particular arrhythmias that are sometimes indistinguishable from the normal heartbeats.

In the ECG records from LTST DB all activities of a tested person during the day are reflected. Moreover, some of these ECG records contain numerous arrhythmias (see ECG signals marked with a 'hash' symbol in table 1). By including these records in our evaluation we actually tested the algorithm in conditions more severe than expected during clinical application of electroporation. The algorithm still worked well if we consider the number of $FP_p$ that appear on arrhythmias in comparison to total number of arrhythmias.

Figure 4 is an example of the correct functioning of our algorithm on ECG signal containing ventricular extrasystoles. EP pulses are not delivered in the case of extrasystoles because they do not satisfy the criteria for a valid QRS complex. Even if they did, the RR interval for extrasystoles would not satisfy the condition for normal heart rate. Moreover, EP pulses are correctly not delivered at normal QRS complexes following the extrasystoles, again due to their RR intervals.
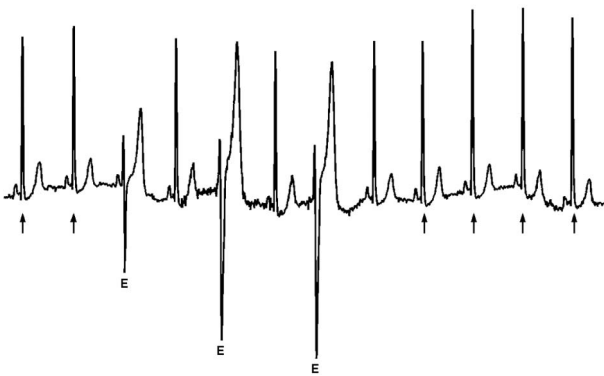


Figure 4. Delivery of EP pulses on ECG signal containing heart arrhythmias (ventricular extrasystoles). The arrows indicate the moments when EP pulses would be delivered. Absence of pulses at three extrasystoles (E) and at three normal QRS complexes following the three extrasystoles demonstrates the ability of the algorithm to prevent the EP pulses from being delivered in case of abnormalities in ECG shape or heart rate. The example belongs to the interval starting at 1:24:17 from the record s20101 of the LTST DB.

The presented algorithm is designed for robust operation in case of ventricular extrasystoles. However, the condition of no ventricular extrasystoles during the learning phase is desirable but not necessary. We tested how the algorithm would work if this condition was not fulfilled (data not shown). We selected four one-minute-long sections from the signal s30752 of the LTST DB which all included ventricular ectopy (phenomenon of seven or more singular ventricular extrasystoles per minute or any run of more than two ventricular extrasystoles). Careful examination of the performance of the developed algorithm on these four sections showed that presence of ventricular extrasystoles either within part I or part II of the learning phase does not affect the performance of the algorithm during the detection and decision-making phase, as long as their number is not very large (for example 10 or more extrasystoles in combination with 10 or fewer normal heartbeats).

## 5. Conclusion

The algorithm for online synchronization of electroporation (EP) pulse delivery with ECG presents a significant improvement over the existing practice of EP delivery with respect to the safety of the patient. This issue is becoming increasingly important because new applications of electrochemotherapy using endoscopic or surgical means to access internal tumours are being developed. Moreover, EP pulses of much longer durations used in some new applications of electroporation (such as electrogene therapy) would more likely coincide with the vulnerable period of the heart muscle if the pulse delivery were not synchronized with the heart activity. Therefore we developed an algorithm that allows EP pulses to be delivered only outside the vulnerable period of the heartbeat and prevents the pulses from being delivered in case of the appearance of some heart arrhythmias such as ventricular extrasystoles. The developed algorithm proved to be an effective tool for QRS detection and EP pulse delivery even in cases of numerous heart arrhythmias, which was confirmed by evaluation of the algorithm on ECG signals of the LTST DB database. The performance of the algorithm is significantly degraded only in presence of disturbances due to body movements that are similar to QRS complex, and in case of extrasystoles, which appear indistinguishable from normal heartbeats.

Implementation of the algorithm in instruments for clinical electroporation would essentially expand the applicability of electrochemotherapy due to a higher level of safety for the patient, as well as the suitability of this method for future applications in anatomical locations presently not yet accessible by existing electroporation devices and electrodes.

## References

1. Heller, R., Jaroszeski, M.J., Reintgen, D.S., Puleo, C.A., DeConti, R.C., Gilbert, R.A. and Glass, L.F., 1998, Treatment of cutaneous and subcutaneous tumors with electrochemotherapy using intralesional bleomycin. *Cancer*, **83**, 148–157.
2. Mir, L.M., Glass, L.F., Serša, G., Teissie, J., Domenge, C., Miklavčič, D., Jaroszeski, M.J., Orlowski, S., Reintgen, D.S., Rudolf, Z., Belehradek, M., Gilbert, R., Rols, M.P., Belehradek Jr, J., Bachaud, J.M., DeConti, R., Štabuc, B., Čemažar, M., Coninx, P. and Heller, R., 1998, Effective treatment of cutaneous and subcutaneous malignant tumors by electrochemotherapy. *British Journal of Cancer*, **77**, 2336–2342.
3. Serša, G., Čufer, T., Čemažar, M., Miklavčič, D., Reberšek, M. and Rudolf, Z., 2000, Electrochemotherapy with bleomycin in the treatment of hypernephroma metastasis: case report and literature review. *Tumori*, **86**, 163–165.
4. Serša, G., Štabuc, B., Čemažar, M., Miklavčič, D. and Rudolf, Z., 2000, Electrochemotherapy with cisplatin: Clinical experience in malignant melanoma patients. *Clinical Cancer Research*, **6**, 863–867.
5. Pucihar, G., Mir, L.M. and Miklavčič, D., 2002, The effect of pulse repetition frequency on the uptake into electropermeabilized cells in vitro with possible applications in electrochemotherapy. *Bioelectrochemistry*, **57**, 167–172.
6. Rols, M.P., Delteil, C., Golzio, M., Dumond, P., Cros, S. and Teissie, J., 1997, In vivo electrically mediated protein and gene transfer in murine melanoma. *Nature Biotechnology*, **16**, 168–171.
7. Bureau, M.F., Gehl, J., Deleuze, V., Mir, L.M. and Scherman, D., 2000, Importance of association between permeabilization and electrophoretic forces for intramuscular DNA electrotransfer. *Biochimica et Biophysica Acta*, **1474**, 353–359.
8. Šatkauskas, S., Bureau, M.F., Puc, M., Mahfoudi, A., Scherman, D., Miklavčič, D. and Mir, L.M., 2002, Mechanisms of in vivo DNA electrotransfer: respective contributions of cell electropermeabilization and DNA electrophoresis. *Molecular Therapy*, **5**, 133–140.
9. Mir, L.M. and Orlowski, S., 1999, Mechanisms of electrochemotherapy. *Advanced Drug Delivery Reviews*, **35**, 107–118.
10. Reilly, J.P., 1998, *Applied Bioelectricity: from Electrical Stimulation to Electropathology* (New York: Springer Verlag).
11. Wiggers, C.J. and Wégria, R., 1940, Ventricular fibrillation due to single, localized induction and condenser shocks applied during the vulnerable phase of ventricular systole. *American Journal of Physiology*, **128**, 500–505.
12. Han, J., 1973, Ventricular vulnerability to fibrillation. *Cardiac Arrhythmias*, 87–95.
13. Hofmann, G.A., 2000, Instrumentation and electrodes for in vivo electroporation. In M.J. Jaroszeski, R. Heller and R. Gilbert (eds), *Electrochemotherapy, Electrogenetherapy, and Transdermal Drug Delivery: Electrically mediated delivery of molecules to cells*, (Totowa, New Jersey: Humana Press), 37–61.
14. Jones, M. and Geddes, L.A., 1977, Strength-duration curves for cardiac pacemaking and ventricular fibrillation. *Cardiovascular Research Center Bulletin*, **15**, 101–112.
15. Ayers, G.M., Alferness, C.A., Ilina, M., Wagner, D.O., Sirokman, W.A., Adams, J.M. and Griffin, J.C., 1994, Ventricular proarrhythmic effects of ventricular cycle length and shock strength in a sheep model of transvenous atrial defibrillation. *Circulation*, **89**, 413–422.
16. Clayton, R.H. and Holden, A.V., 2000, Re-entry in computational models of heterogenous and abnormal myocardium. *International Journal of Bioelectromagnetism*, **2(2)**, http://www.ijbem.org/volume2/number2/clayton/paper_ijbem.htm (last accessed on 22 December 2004).
17. Guyton, A.C. and Hall, J.E., 1996, Textbook of Medical Physiology (Pennsylvania: W.B. Saunders Company).
18. Friesen, G.M., Jannett, T.C., Jadallah, M.A., Yates, S.L., Quint, S.R. and Nagle, H.T., 1990, A comparison of the noise sensitivity of nine QRS detection algorithms. *IEEE Transactions on Biomedical Engineering*, **37**, 85–98.
19. Benitez, D.S., Gaydecki, P.A., Zaidi, A., Fitzpatrick, A.P. and Laguna, P., 2000, A new QRS detection algorithm based on the Hilbert transform. *IEEE Computers in Cardiology*, **27**, 379–382.
20. Hamilton, P.S. and Tompkins, W.J., 1986, Quantitative investigation of QRS detection rules using the MIT/BIH arrhythmia Database. *IEEE Transactions on Biomedical Engineering*, **33**, 1157–1165.
21. Laguna, P., Jané, R. and Caminal, P., 1994, Automatic detection of wave boundaries in multilead ECG signals: Validation with the CSE Database. *Computers and Biomedical Research*, **27**, 45–60.
22. Pan, J. and Tompkins, W.J., 1985, A real-time QRS detection algorithm. *IEEE Transactions on Biomedical Engineering*, **32**, 230–236.
23. Jager, F., 2002, Feature extraction and shape representation of ambulatory electrocardiogram using the Karhunen-Loève transform. *Electrotechnical Review*, **69**, 83–89.
24. Jager, F., Taddei, A., Moody, G.B., Emdin, M., Antolič, G., Dorn, R., Smrdel, A., Marchesi, C. and Mark, R.G., 2003, Long-Term ST Database: a reference for the development and evaluation of automated ischaemia detectors and for the study of the dynamics of myocardial ischaemia. *Medical & Biological Engineering & Computing*, **41**, 172–182.
25. Ruha, A., Sallinen, S. and Nissilä, S., 1997, A real-time microprocessor QRS detector system with a 1-ms timing accuracy for the measurement of ambulatory HRV. *IEEE Transactions on Biomedical Engineering*, **44**, 159–167.